ENVIRONMENTAL RESEARCH
COMMUNICATIONS

INCLUSIVE PUBLISHING TRUSTED SCIENCE

Part of the ENVIRONMENTAL RESEARCH SERIES

PURPOSE-LED PUBLISHING™

LETTER • OPEN ACCESS

Stratification and wind changes shape future Indian Ocean chlorophyll

To cite this article: Kwatra Sadhvi *et al* 2026 *Environ. Res. Commun.* **8** 011004

Environmental Research Communications

OPEN ACCESS

RECEIVED
12 August 2025

REVISED
11 December 2025

ACCEPTED FOR PUBLICATION
6 January 2026

PUBLISHED
15 January 2026

LETTER

Stratification and wind changes shape future Indian Ocean chlorophyll

Kwatra Sadhvi[1,*], **Matthieu Lengaigne**[2], **Iyyappan Suresh**[1,3], **Cyril Dutheil**[2] and **Jérôme Vialard**[4]

[1] Digital University Kerala (DUK), Trivandrum, India
[2] MARBEC, IFREMER, IRD, University of Montpellier, Montpellier, France
[3] CSIR- National Institute of Oceanography, Goa, India
[4] LOCEAN/IPSL, Sorbonne Universités (UPMC, Université Paris 06)-CNRS-IRD-MNHN, Paris, France
[*] Author to whom any correspondence should be addressed.

E-mail: sadhvik16@gmail.com

Keywords: Indian Ocean, climate change, surface chlorophyll, stratification, upwelling, wind changes

Supplementary material for this article is available online

Abstract

Large uncertainties in projected future changes of Indian Ocean chlorophyll across Earth System Models are largely attributed to differences in biogeochemical process representation. We show, however, that large biases in the historical physical state of the ocean and inter-model differences in future climate also play a substantial role. Using a bias-corrected ocean-only model forced by air-sea flux anomalies from multiple CMIP6 models, we find that correcting historical physical state biases amplify projected summer surface chlorophyll (SChl) changes by up to a factor of two and improves inter-model consistency. Heat flux driven enhanced upper ocean stratification, consistently reduces SChl by −10% to −40%, depending on the upwelling region. Wind-driven nutricline changes dominate responses in SChl, off southern India (−45% wind effect versus −30% from stratification) and Sumatra (+25% versus −12%). These results highlight the need to improve the representation of monsoonal winds and their future evolution to better constrain biogeochemical projections.

1. Introduction

The Indian Ocean experiences the strongest monsoonal wind forcing among all tropical basins, driving vigorous coastal and open-ocean upwelling during the summer monsoon. These upwelling transport nutrient-rich waters to the surface, fueling some of the most intense phytoplankton blooms in the tropics (Wiggert *et al* 2005, Lévy *et al* 2007, Hood *et al* 2024). These blooms are fundamental to sustaining the marine food web and contributing to the Indian Ocean's status as the second-largest source of economically valuable tuna catches globally (Lecomte *et al* 2017). As such, surface chlorophyll (SChl)—a satellite-observable proxy for phytoplankton biomass—is a key indicator of primary productivity and ecosystem health in the region (Friedland *et al* 2012).

Since the advent of satellite observations in 1998, observational studies have reported declining SChl trends across various parts of the basin, though the spatial patterns are heterogeneous depending on the product and period analyzed (Siegel *et al* 2013, Gregg and Rousseaux 2014, Roxy *et al* 2016, Dunstan *et al* 2018, Gregg and Rousseaux 2019, Hammond *et al* 2020, Modi and Roxy 2023, Yu *et al* 2023). The longest continuous satellite-derived record to date (25 years) reveals a significant SChl decline in the northwestern Arabian Sea but localized increases in the eastern Indian Ocean—particularly off Sumatra, Java, and within the Sri Lankan upwelling zone (Modi and Roxy 2023). This basin-wide decline coincides with long-term warming trends in the Indian Ocean, which are largely attributed to anthropogenic forcing (Dong *et al* 2014). Several studies have therefore attributed this general Indian Ocean SChl decline to anthropogenic climate change (Pathinara *et al* 2024, Roxy

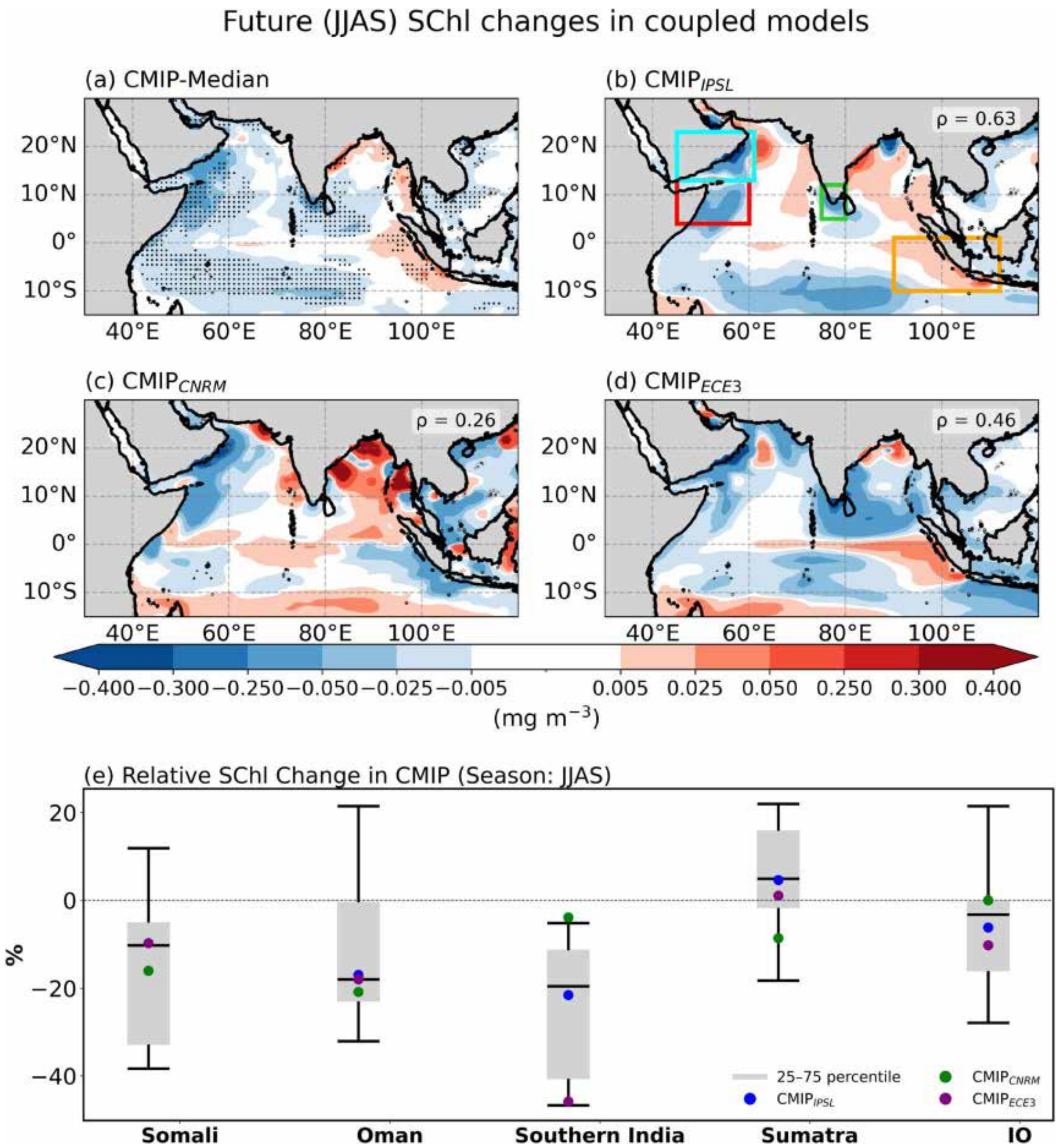

Figure 1. Projected summer (June–September; JJAS) changes in surface chlorophyll (SChl, mg m^{-3}) at the end-of-century (2068–2087) relative to present (1948–1967). Maps show changes from the: (a) CMIP multi-model median (see table S1 for the list of models; the median offers a more robust central estimate: Laufkötter *et al* 2015; Anugerahanti *et al* 2018), (b) CMIP$_{IPSL}$, (c) CMIP$_{CNRM}$ and (d) CMIP$_{ECE3}$ coupled models. Stipplings indicate where more than 70% of models agree on the sign of the change. Spearman rank correlation coefficients (ρ) in panels (b–d) quantify the spatial agreement between each model's SChl change pattern and the CMIP-Median shown in (a). Note the nonlinear color scale for panels (a)–(d). (e) Distribution of projected SChl changes across CMIP models in several key regions (see panel b). IO domain [15°S–30°N; 30°E–114°E]. Changes are expressed as a percentage relative to each model's historical baseline value. The black horizontal line shows the median, box edges represent the 25th and 75th percentiles, whiskers the 10th and 90th percentiles, and colored dots indicate the CMIP$_{IPSL}$ (blue), CMIP$_{CNRM}$ (green) and CMIP$_{ECE3}$ (purple) values.

et al 2016) even though it remains difficult to disentangle the impact of anthropogenic forcing from that of natural climate variability. (Henson *et al* 2016, Tian and Zhang 2023).

Projections from the latest generation of Earth System Models in Coupled Model Intercomparison Project 6 (CMIP6) broadly align with observed trends—predicting a widespread decline in surface chlorophyll (SChl) across the tropical Indian Ocean, especially in the western Arabian Sea and near the southern tip of India (figures 1(a), (e); Tian and Zhang 2024). However, they also indicate localized increases along the west coasts of Java and Sumatra (figures 1(a), (e), Modi and Roxy 2023). This average decline masks considerable inter-model spread (figure 1(e)), which limits confidence in the projections (Tagliabue *et al* 2021).

A significant part of the inter-model differences is suspected to stem from limitations in the representation of biogeochemical process, such as nitrogen fixation, iron limitation, and zooplankton grazing (e.g., Bopp *et al* 2013, Kwiatkowski *et al* 2020). Yet recent studies suggest that physical factors—particularly large biases in the historical mean state—also play a significant role (e.g., Lachkar *et al* 2018, Praveen *et al* 2020, Tagliabue *et al*

2021, Modi and Roxy 2023). In particular, the difficulty in simulating monsoonal winds, combined with error amplification from air-sea coupling, results in systematic biases in coupled climate models, such as overly weak zonal surface winds near the equator (easterly wind bias) and a cold bias in the northern Indian Ocean (Li *et al* 2015, Feng *et al* 2023, Mohanty *et al* 2024). These errors affect the simulation of historical productivity and may distort projections of future change. The first goal of this study is to assess whether such physical biases also contribute to biased SChl projections.

Widespread SChl declines in the Indian Ocean and other tropical regions have largely been attributed to enhanced upper-ocean stratification caused by surface warming, which reduces vertical mixing and nutrient supply to the euphotic zone (Behrenfeld *et al* 2006, Roxy *et al* 2016). However, regional wind-driven changes can also strongly modulate nutrient availability and chlorophyll distributions, particularly in equatorial and coastal upwelling zones (Praveen *et al* 2016, Parvathi *et al* 2017, Lachkar *et al* 2018, Praveen *et al* 2020). For example, models consistently project a weakening of the Indo-Pacific Walker circulation (e.g., Vecchi *et al* 2006), leading to easterly wind anomalies and a flatter thermocline over the equatorial Indian Ocean. While all models simulate future surface warming and enhanced stratification in the Indian Ocean (Dong *et al* 2014), the strength of Walker circulation weakening varies considerably across models (Gopika *et al* 2025). Wind changes can also lead to both increases and decreases in productivity depending on regional patterns. In this context, the second goal of our study is to quantify the relative contributions of stratification (driven by heat and freshwater fluxes) and circulation (wind-driven) changes to SChl future changes. This aspect has, to our knowledge, not yet been addressed.

Here, we use a novel ocean-only modeling framework that applies future surface flux changes from CMIP6 models to bias-corrected historical simulations with minimized mean-state errors (Lengaigne *et al* 2024). We apply this approach to flux changes from three representative CMIP6 models and from multi-model mean (MMM) of fifteen CMIP6 models to isolate the physical drivers of future summer SChl changes in the Indian Ocean. This approach allows us to: (1) assess how historical model biases influence projected SChl changes; (2) disentangle the roles of surface heat, momentum, and freshwater fluxes using targeted sensitivity experiments; and (3) identify the dominant physical drivers of inter-model differences. The rest of the paper is organized as follows. Section 2 summarizes the methodology. In section 3, we evaluate the impact of correcting historical biases in the mean state on SChl projections. Section 4 quantifies the respective contributions of stratification (heat and freshwater-driven) and circulation (wind-driven) changes in oceanic state, and examines model dependence. Section 5 discusses the broader implications of our results in light of previous studies.

2. Data and methods

We analyze biogeochemical outputs from 13 CMIP6 (Eyring *et al* 2016) Earth System Models (marked by †, table S1) that provide both historical and SSP5-8.5 simulations. Models were selected based on the availability of monthly SChl outputs. Simulated SChl is evaluated against the ESA Ocean Colour Climate Change Initiative (OC-CCI) version 3.1 SChl dataset, which merges observations from SeaWiFS, MODIS, MERIS, and VIIRS sensors for the 1998–2016 period (Sathyendranath *et al* 2018). We focus on the summer monsoon season (June–September, JJAS), which marks the annual peak in biological productivity (Lévy *et al* 2007). For all CMIP6-based projected changes, we define future anomalies as the difference between 2068–2087 and a 1948–1967 historical baseline. When comparing model output with observations, we instead use 1998–2016, corresponding to the satellite era. Sensitivity tests using 30- or 50-year averaging windows produce similar patterns and amplitudes, indicating that our conclusions are not sensitive to the precise averaging period (not shown).

To isolate the physical drivers of future SChl changes and reduce historical model biases, we adopt the ocean-only framework of Lengaigne *et al* (2024) (figure 2), implemented with the NEMO-PISCES ocean biogeochemical model (Supplementary Information Text S1 and figure S1). In this setup, long-term changes in surface heat, momentum, and freshwater fluxes from historical and future simulations are added to a control simulation (hereafter noCC; figure 2 and table S2 for the list of experiments), which is forced by detrended JRA-55 reanalysis fluxes. Detrending removes the anthropogenic climate change signal, while the JRA-55 fluxes - being observationally constrained - are largely free from the systematic biases present in CMIP6 models; hence the term ‘corrected’ simulations.

To generate corrected climate change experiments (CC-COR), anomalies associated with anthropogenic changes in surface heat, momentum and freshwater fluxes diagnosed from selected CMIP6 models are superimposed onto the noCC forcing (figure 2 and table S2). Heat flux changes are separated into (1) Sea Surface Temperature-independent components, such as cloud-induced solar changes and effects of wind and relative humidity on evaporation and (2) Sea Surface Temperature-dependent feedbacks, including variations in latent heat and longwave radiation linked to Sea Surface Temperature anomalies. The former are added directly; the

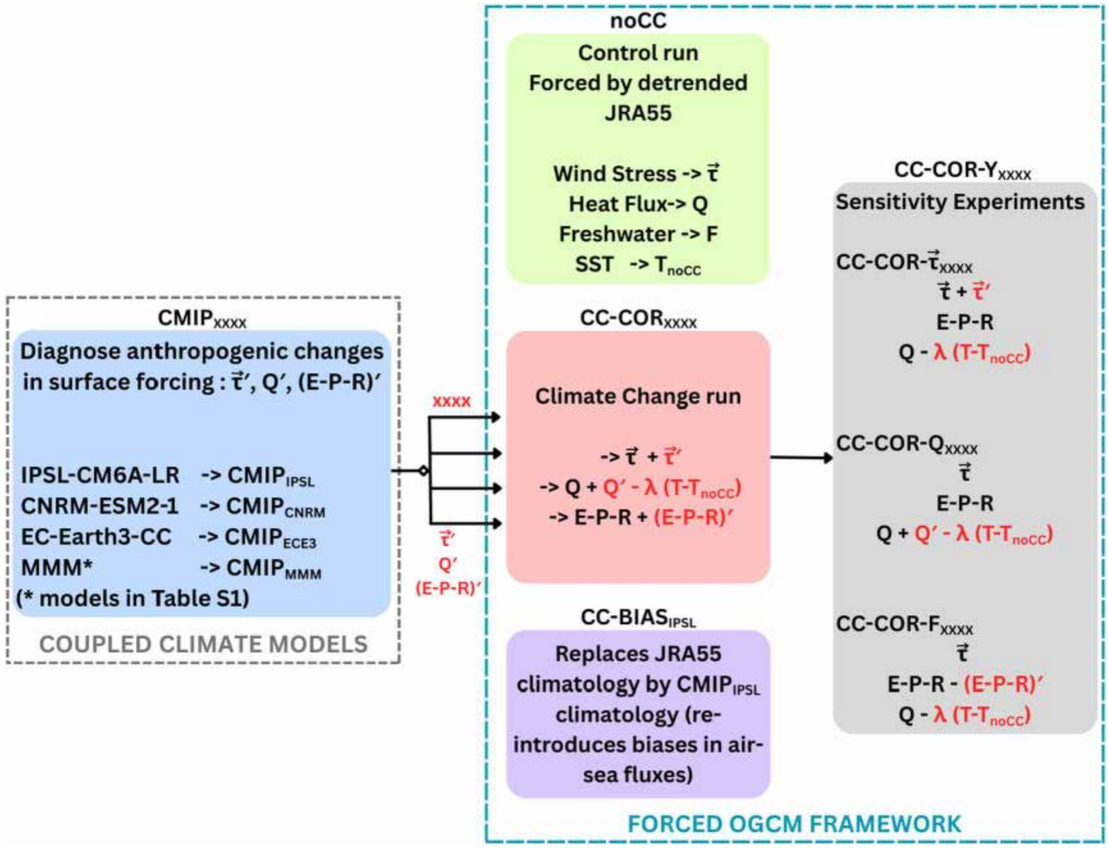

Figure 2. Schematic of the experimental forcing strategy and nomenclature used in this study. Anthropogenic surface-forcing anomalies (wind stress τ', heat flux Q', and freshwater flux (E–P–R)′) are diagnosed from multiple CMIP models and applied to an ocean-only model framework. The noCC simulation is a bias-corrected control forced by detrended JRA55 fields, while CC-COR applies the full set of climate-change anomalies. Sensitivity experiments (CC-COR-τ, CC-COR-Q, CC-COR-F) isolate the individual contributions of wind, heat, and freshwater forcing, respectively. The CC-BIAS experiment replaces JRA55 climatology with CMIP-derived climatology to reintroduce air–sea flux biases. Details in table S2.

latter are applied as a relaxation to the noCC Sea Surface Temperature, following the physically justified approach of Lengaigne *et al* (2024).

The climate change response is obtained from CC-COR minus noCC. Additional sensitivity experiments isolate the individual contributions from each flux type: momentum (CC-COR-τ), heat (CC-COR-Q) and freshwater (CC-COR-F). For example, CC-COR-τ minus noCC isolates the response of future wind stress changes in a bias corrected configuration.

We use outputs from four selected CMIP6 Earth System Models to obtain future surface flux forcing: IPSL-CM6A-LR, CNRM-ESM2–1, EC-Earth3-CC (hereafter, $CMIP_{IPSL}$, $CMIP_{CNRM}$ and $CMIP_{ECE3}$, respectively). These models were chosen for their consistency with our framework, as they share the same ocean physical and biogeochemical configuration based on NEMO-PISCES. While they do not span the full range of projected summer SChl changes in the Somali and Oman upwelling regions, they cover a wide spread for Sumatra and southern India (figure 1(e)).

We also constructed a future surface flux forcing based on the multi-model mean (MMM) of 15 (marked by a * in table S1) CMIP6 models. This provides a more representative estimate of the inter-model consensus on future air-sea flux changes than any single model.

With a pattern correlation of 0.63, the $CMIP_{IPSL}$ projection closely matches the 13 CMIP6 models' († , table S1) multi-model median (figures 1(a), (b), (e)) and is thus discussed first. For this model, we conduct additional control (noCC-$BIAS_{IPSL}$) and climate change (CC-$BIAS_{IPSL}$) simulations in which the JRA-55 seasonal climatology is replaced by that of $CMIP_{IPSL}$, thereby reintroducing coupled model biases (figure 2). To validate our forced approach, we compare $CMIP_{IPSL}$ coupled projections with their biased forced counterpart (CC-$BIAS_{IPSL}$). Projected changes in physical variables are nearly identical in both cases (not shown). Summer monsoon (JJAS) SChl are also very similar, both in term of historical mean state (figures S2(a), (b)) and future projections (Figures S2(c), (d)). We therefore, will compare the forced CC-$BIAS_{IPSL}$ and CC-COR_{IPSL} simulations to assess the impact of bias correction (see section 3).

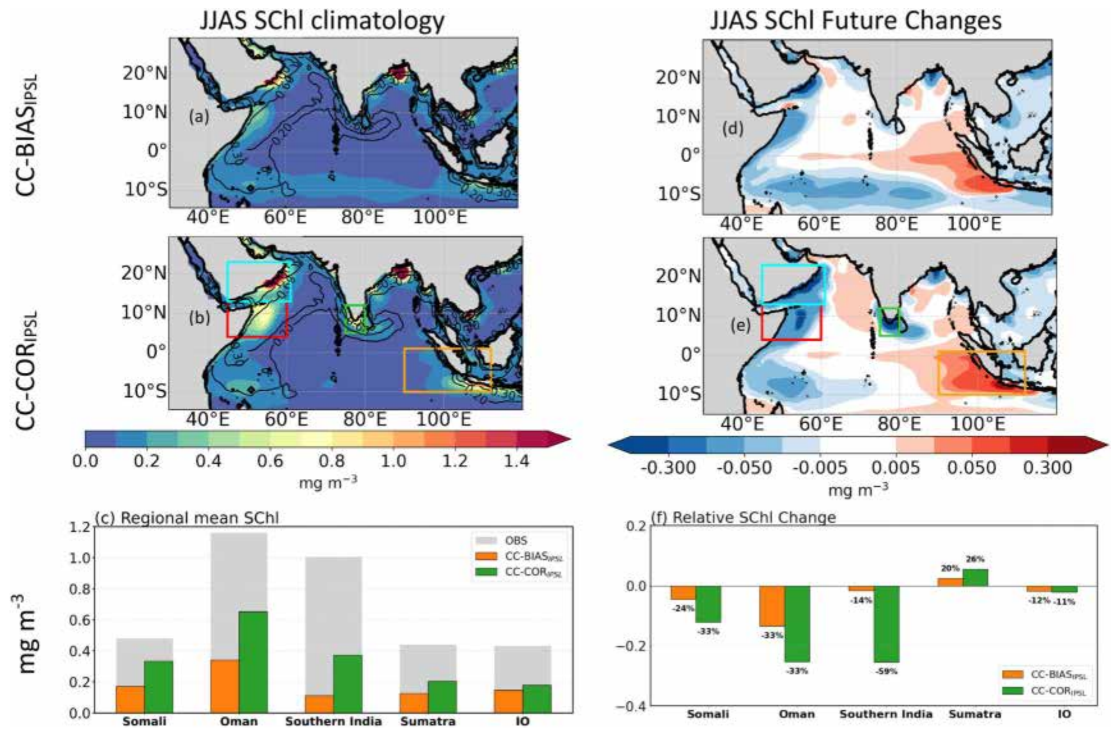

Figure 3. Summer (June–September; JJAS) surface chlorophyll (SChl, mg m^{-3}) from 1998–2016 and projected end-of-century changes. (a)–(b) Climatological JJAS SChl from the (a) CC-BIAS$_{IPSL}$ and (b) CC-COR$_{IPSL}$ experiments; contours in black indicate the observed JJAS climatology. (c) Regional averages of climatological SChl in key regions (see panels b, e) from CC-BIAS$_{IPSL}$ (orange), CC-COR$_{IPSL}$ (green), and observations (grey). (d)–(e) Projected end-of-century changes in SChl from the (d) CC-BIAS$_{IPSL}$, and (e) CC-COR$_{IPSL}$ experiments. (f) Regional averages of projected changes from CC-BIAS$_{IPSL}$ (orange), CC-COR$_{IPSL}$ (green). Bars show future changes; percentages indicate relative changes with respect to control values. Upwelling regions are marked in panels (b) and (e): Somali (red), Oman (cyan), Southern India (green), and Sumatra (orange). IO domain [15°S–30°N; 30°E–114°E]. Differences between CC-BIAS$_{IPSL}$ and CC-COR$_{IPSL}$ highlight the contribution of physical mean-state biases in CMIP$_{IPSL}$ on SChl projections. Note the nonlinear color scale for panels d and e.

3. Results

3.1. Impact of historical model biases on chlorophyll projections

We first evaluate whether our ocean-only framework effectively reduces historical biases, using CMIP$_{IPSL}$ as a representative case. Both the CC-BIAS$_{IPSL}$ (figure 3(a)) and CC-COR$_{IPSL}$ (figure 3(b)) simulations capture the observed large-scale patterns of summer phytoplankton blooms (Figure S3(c)), particularly in major upwelling regions of Somalia, Oman, southern India, and Sumatra (figures 3(a), (b); Figure S2(a), (b)). However, both simulations substantially underestimate SChl concentrations—by a factor of two or more—in key upwelling regions (figure 3(c)). For instance, the observed SChl exceeds ~1.1 mg m^{-3} in the Oman region, while CC-BIAS$_{IPSL}$ simulates 0.5 mg m^{-3}. Correcting air-sea flux biases in IPSL-CM6A-LR (CC-COR$_{IPSL}$) increases bloom amplitudes by 30%–100% (figure 3(c)). This highlights that mean-state physical biases in CMIP$_{IPSL}$ contribute substantially to the underestimation of SChl. Despite this improvement, SChl remains under-estimated. This indicates that missing submesoscale processes or imperfect biogeochemical parameterizations also contribute to model–observational data discrepancies. Additional validations (Figures S3, S4 and S5) further demonstrate that the bias-corrected simulation reproduces the SChl and mixed layer depth observed climatology, seasonal cycle, and interannual variability more faithfully than the CMIP$_{IPSL}$ model.

We next examine how these corrections affect future projections. The corrected simulation (CC-COR$_{IPSL}$) projects substantially larger SChl changes—often more than double those in the biased simulation (figure 3(f)), with a particularly large impact off South India (from −0.05 mg m^{-3} to −0.27 mg m^{-3} in the corrected simulation). The impact of the correction is smaller when changes are expressed in percentage of the historical value (numbers above bars on figure 3(f)), but remain higher in the corrected simulation, especially off South India (−14% versus%−59%).

These results underscore the strong sensitivity of projected summer SChl responses to historical physical biases and demonstrate the importance of bias correction for improving confidence in climate-driven biogeochemical projections. Figure S6 confirms this across all forcing datasets (IPSL, CNRM, and ECE3). To further interpret these changes, figure S7 shows that the largest relative declines occur for diatoms, whereas nanophytoplankton exhibit much weaker relative changes, consistent with a shift toward smaller phytoplankton in

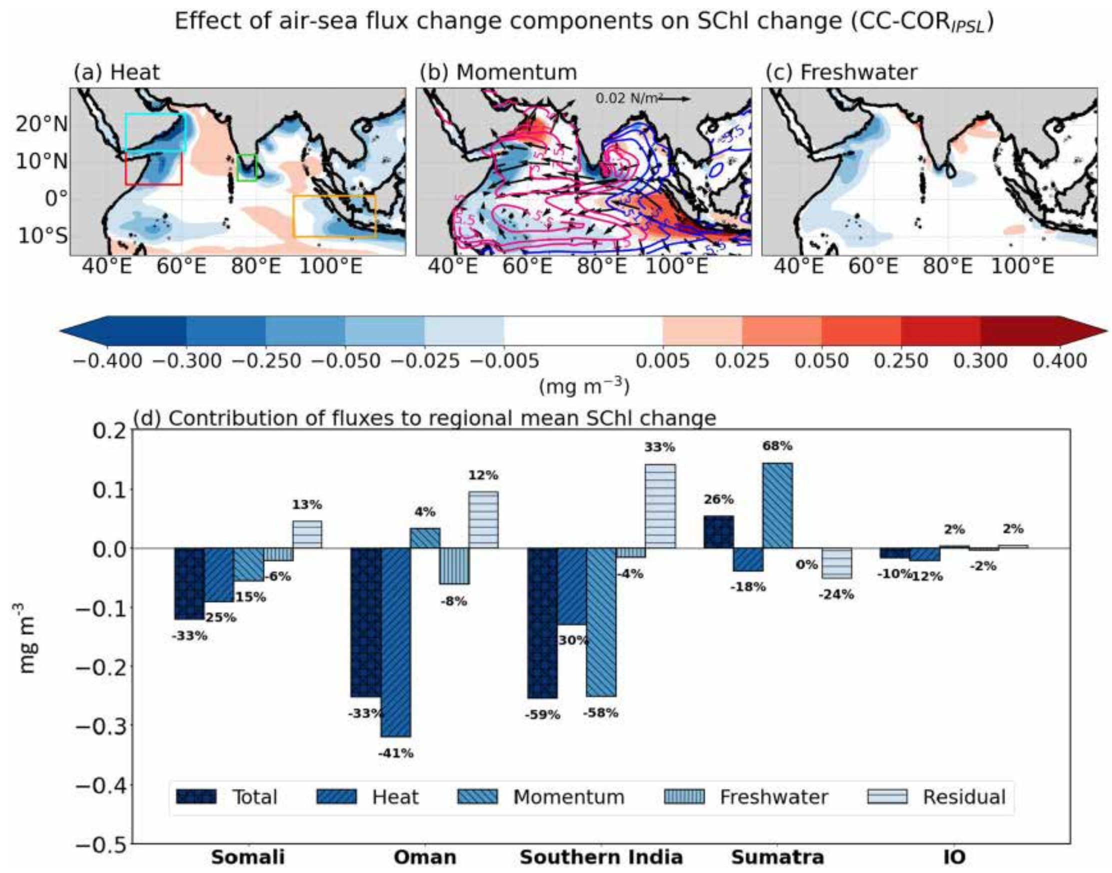

Figure 4. Projected summer (June–September; JJAS) future changes in surface chlorophyll (SChl, mg m^{-3}) at the end-of-century from sensitivity experiments isolating the effects of individual air-sea flux components in the CC-COR$_{IPSL}$ setup. Contributions from: (a) heat (CC-COR-Q$_{IPSL}$), (b) momentum (CC-COR-τ_{IPSL}), and (c) freshwater (CC-COR-F$_{IPSL}$) fluxes (see methods for details). (d) Regionally-averaged SChl changes from the corrected experiment, decomposed into heat, momentum, freshwater and a residual term representing nonlinear interactions. Upwelling regions are outlined in panel (a): Somali (red), Oman (cyan), Southern India (green), and Sumatra (orange). IO domain [15°S–30°N; 30°E–114°E]. Bars show future changes; percentages indicate changes relative to historical baseline values. Contours in panel (b) show changes in relative sea level anomalies (a proxy for thermocline and nutricline depth changes: red for positive and blue for negative) in the CC-COR-τ_{IPSL} experiment. Note the nonlinear color scale for panels (a)–(c). All percentage values below the zero line in (d) are negative.

warmer climates (e.g., Bopp *et al* 2013, Kwiatkowski *et al* 2020). In the next section, we disentangle the individual contributions of heat, momentum, and freshwater fluxes to projected SChl changes in the bias-corrected simulations.

3.2. Stratification and circulation as drivers of future chlorophyll changes

Figure 4 shows the breakdown of projected SChl changes into contributions from surface heat, momentum (wind stress), and freshwater fluxes, based on CC-COR$_{IPSL}$ projections. This decomposition helps distinguish the effects of stratification—primarily driven by heat and freshwater fluxes—from those of ocean circulation, which is mainly driven by wind stress. Among these, heat and momentum fluxes dominate across all upwelling regions, while freshwater fluxes have a negligible impact (figure 4(d)).

There is a residual, associated with nonlinear interactions between the responses to various fluxes (figure S8(b)). Those nonlinear interactions consistently act as damping (i.e., they reduce the total SChl change compared to the sum of individual contributions). Though typically smaller than the leading driver, these nonlinear effects are non-negligible in some regions and are revisited in the discussion section (figure 4(d)).

Surface warming, attributable to heat flux changes (figure S1), enhances upper-ocean stratification and suppresses vertical nutrient supply (figure S9; Behrenfeld *et al* 2006), leading to widespread SChl declines—especially in upwelling regions (figure 4(a)). Heat fluxes alone account for 20%–40% reductions (figure 4(d)) in these regions and are the primary driver of projected Schl changes in the Somali and Oman upwellings.

Momentum flux changes have a more heterogeneous influence (figure 4(b)). Wind stress leads to a declines of 15% off Somalia and 60% in southern India, a ~70% increase off Sumatra, and minimal change off Oman. These wind-driven circulation changes dominate the total SChl response off southern India (where they reinforce stratification effects) and off Sumatra (where they counteract them and produce a net increase; figure 4(d)).

The spatial patterns of wind-driven SChl changes closely follow anomalies in relative sea level (figure 4(b)), a proxy for thermocline and nutricline displacement. It is computed by removing the basin-wide mean sea level. Negative values (shoaling nutricline, see figure S10) correspond to SChl increases; positive values (deepening nutricline) to decreases. Easterly equatorial wind anomalies—linked to a weakened Walker circulation projected in many CMIP6 models (e.g., Held and Soden 2006, Sharma *et al* 2022)—shoal the thermocline and nutricline (figure S10) in the eastern equatorial Indian Ocean and deepen it in the west (figure 4(b)). This enhances upwelling off Sumatra and suppresses it in the southwestern Arabian Sea. Off southern India, easterly anomalies drive coastal downwelling (Suresh *et al* 2018) and onshore Ekman transport, deepening the thermocline (Parvathi *et al* 2017), nutricline (figure S10) and reducing SChl (figure 4(b)). The weak momentum-driven response in the Oman upwelling likely results from a balance between upwelling-favorable coastal winds and opposing downwelling-favorable winds to the south.

To test the robustness of these results, we extended the analysis to bias-corrected simulations forced with flux anomalies from $CMIP_{CNRM}$, $CMIP_{ECE3}$, and the $CMIP_{MMM}$ (figure 5). Given the negligible role of freshwater fluxes, we focus on heat and momentum. Across all forcing sets, increased heat fluxes consistently enhance thermal stratification and reduce nutrient supply (figure S10), leading to robust SChl declines (figure 5(e)). Except for the Oman upwelling, these reductions are remarkably consistent across models: on average ∼−15% off Sumatra, −20% off Somalia, −30% off southern India, and −35% off Oman.

In contrast, wind-driven effects show greater spatial and inter-model variability. All models project easterly anomalies off southern India, consistently inducing SChl declines (−38% to −61%) via downwelling-favorable conditions. However, off Sumatra, projected changes vary widely—from a strong increase in $CC\text{-}COR_{IPSL}$ (figure 5(a)) to a slight decrease in $CC\text{-}COR_{CNRM}$ (figure 5(b)). These differences reflect variations in equatorial wind strength and local alongshore winds. For example, $CC\text{-}COR_{IPSL}$ features strong equatorial easterlies and upwelling-favorable coastal winds, promoting nutricline shoaling and a robust SChl increase (figures 5(a), (f)). By comparison, $CC\text{-}COR_{CNRM}$ shows weaker equatorial anomalies resulting in modest thermocline deepening and a weak SChl increase (figures 5(b), (f)). Momentum-driven changes in the Somali and Oman upwellings also vary across model forcing sets, reflecting local differences in wind patterns.

Overall, enhanced stratification due to heat fluxes drives a consistent reduction in SChl across all Indian Ocean upwelling regions, with the strongest effects in the AS upwelling regions (figure 5(e)). In contrast, wind-driven circulation changes dominate the total SChl response in the southern India and Sumatra upwellings and largely explain the inter-model spread in those regions (figure 5(f)).

4. Summary and discussion

Projections of phytoplankton and primary production from Earth System Models remain highly uncertain, particularly in the Indian Ocean (Tagliabue *et al* 2021). Part of this uncertainty stems from differences in the representation of biogeochemical processes across models, including nitrogen fixation (Bopp *et al* 2022), iron limitation (Tagliabue *et al* 2020), and zooplankton grazing (Moffett and Landry 2020). While wind-driven circulation has also been suggested as a key driver (e.g., Lachkar *et al* 2018, Praveen *et al* 2020, Modi and Roxy 2023), its contribution to projection uncertainty has been poorly quantified. Using a controlled ocean-only framework, we show that correcting for historical mean-state biases can amplify projected surface chlorophyll (SChl) changes by up to a factor of two.

Targeted sensitivity experiments provide a mechanistic understanding of the projected changes. Consistent with earlier studies (e.g., Behrenfeld *et al* 2006, Roxy *et al* 2016), we find that surface warming enhances upper-ocean stratification, reducing vertical nutrient supply and causing widespread SChl declines across upwelling regions. However, our results also reveal an interplay between thermally driven stratification and wind-driven circulation (see figure S11 for a schematic illustration). The effect of stratification changes dominates in the Somali and Oman upwellings, while that of circulation changes is the main driver in the southern India and Sumatra regions. These wind-driven effects are linked to a projected weakening of the Walker circulation (e.g., Held and Soden 2006, Sharma *et al* 2022), which alters thermocline depth and nutrient supply, but regional wind anomalies also play a substantial role. Although Earth System Models generally project a weakening of monsoonal winds (Sooraj *et al* 2015, Parvathi *et al* 2017), the spatial variability in wind changes strongly influences both the magnitude—and, in some cases, the sign—of SChl responses in these regions. Notably, the diversity of wind projections across models contributes significantly to the spread in regional SChl responses.

The nonlinear effects arising from the combined forcing by heat, momentum, and freshwater flux forcing warrant further attention. Although smaller than the primary drivers emphasized here, these nonlinearities are consistently non-negligible (figure 4(d); figure S8), reflecting the intrinsically nonlinear nature of physical and

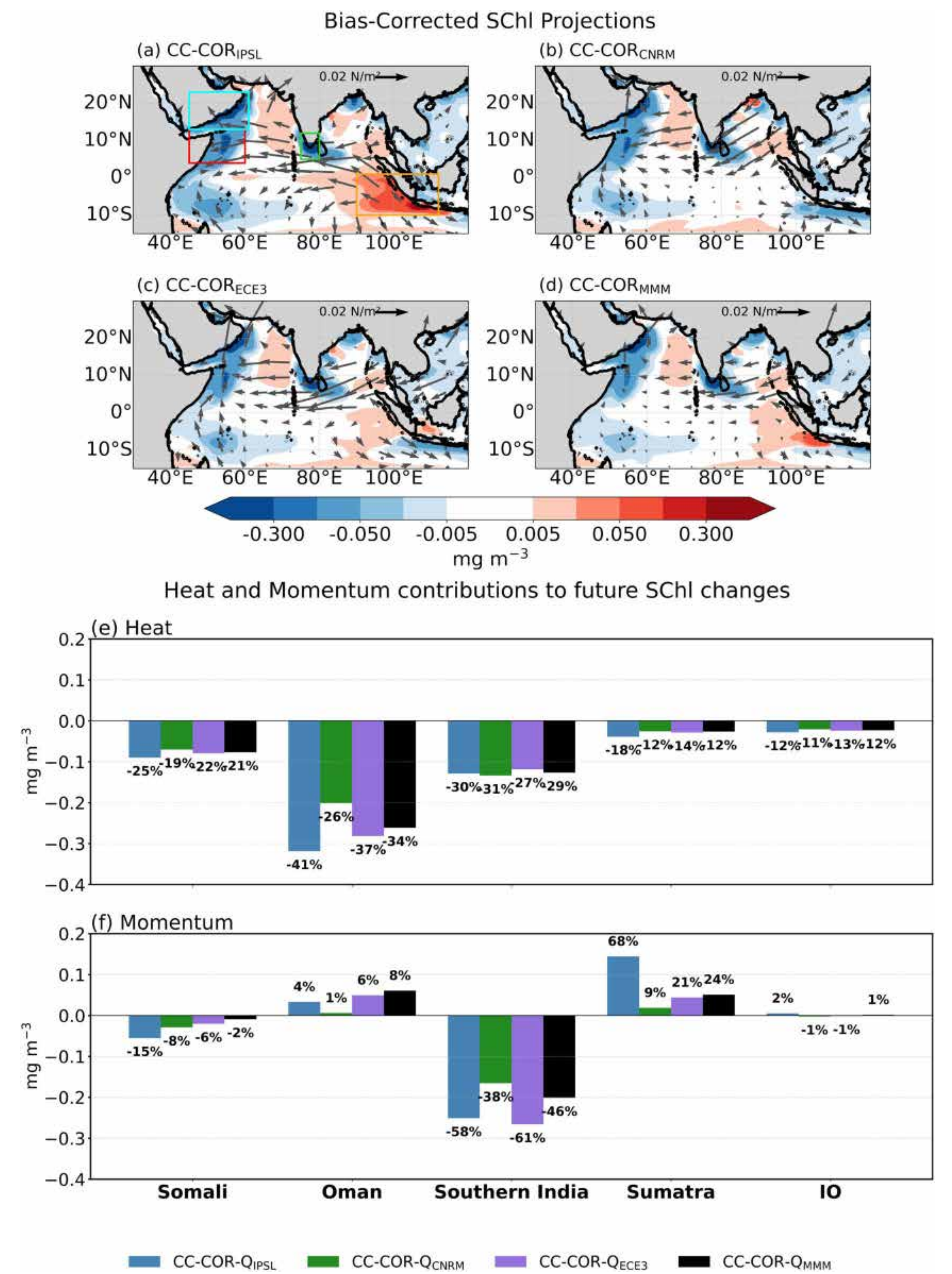

Figure 5. Projected summer (June–September) changes in surface chlorophyll (SChl, mg m^{-3}) at the end-of-century. SChl changes from (a) CC-COR$_{IPSL}$, (b) CC-COR$_{CNRM}$, (c) CC-COR$_{ECE3}$ and (d) CC-COR$_{MMM}$ simulations. Shading indicates SChl change, and arrows show changes in surface wind stress. (e)–(f) Contributions of (e) heat and (f) momentum flux changes to each model's regional SChl response, averaged over key upwelling regions (Somali, Oman, Southern India, and Sumatra, see panel (a) and IO domain [15°S–30°N; 30°E–114°E]. Bars represent future changes; percentages indicate changes relative to historical baseline values. Note the non-linear color scale for panels (a)–(d).

biogeochemical processes. For instance, nutrient co-limitations can cap SChl increases even when nutrient supply rise, while reduced zooplankton grazing can partly offset SChl declines. Similarly, mixing processes are inherently nonlinear, so wind- and stratification-driven changes in nutrient availability do not simply add together. While our sensitivity experiments isolate the dominant contributions of heat and momentum fluxes, these nonlinear interactions highlight the importance of jointly considering stratification and circulation changes when interpreting regional SChl responses.

A key limitation of our study is that the bias-corrected simulations still underestimate summer SChl by 30%–60% in major upwelling regions (figure 3(c)). Our results show that projected changes remain highly sensitive to the historical baseline mean state—even when expressed as relative anomalies (figure 3(f)). This underestimation likely stems from a combination of factors, including unresolved submesoscale and mesoscale variability (Resplandy *et al* 2011), limitations in biogeochemical parameterizations, and remaining errors in the JRA-55 forcing and ocean model physics. As a result, the absolute magnitude of projected SChl in upwelling regions may still be conservative, even though the relative (percentage) changes are consistent across models. Absolute projections should therefore be interpreted with caution until historical physical and biogeochemical biases are further reduced. Addressing this issue will require targeted experiments exploring the role of model resolution and biogeochemical parameterizations.

Another limitation of our approach is that the future air–sea flux changes are taken from three individual models that share nearly identical ocean physical and biogeochemical components (NEMO–PISCES). While these models capture a wide range of SChl responses in the Southern India and Sumatra upwellings, where wind effects dominate, they span only a narrow range of outcomes in the Somali and Oman upwellings. This restricted spread likely reflects a greater sensitivity to biogeochemical process representation in the western Arabian Sea. Because all three forcing models employ PISCES as their biogeochemical core, the sampled diversity is limited. A more comprehensive assessment using models with distinct biogeochemical formulations will be essential to fully characterize the relative roles of biogeochemical parameterizations and wind-projection uncertainty in this region.

In addition, our framework only corrects the mean-state biases, but does not account for potential errors in the future changes in air-sea fluxes. Those heat flux changes are indeed simply taken from CMIP models and therefore inherit any biases in their projected responses to greenhouse-gas forcing. This may lead to misrepresentations of how stratification, temperature, or circulation changes translate into SChl variability. A more complete approach would require an emergent constraint approach to correct future changes in surface heat fluxes (similar to the approach in Li *et al* 2016) or a flux-correction strategy implemented within a fully coupled ocean–atmosphere model (e.g., Zhuo *et al* 2025). Such an approach would provide a more refined assessment of how CMIP biases in both historical climatology and climate-change response affect projected biogeochemical responses in the Indian Ocean.

Overall, our results underscore the need for improved simulation of monsoonal wind systems and their teleconnections—particularly the Walker circulation—in future generations of coupled climate models. They also support calls for bias-aware ensemble frameworks (Seelanki and Pant 2021, Mohanty *et al* 2024) and process-based model evaluation strategies (Long *et al* 2020) to better constrain marine biogeochemical projections under climate change.

Acknowledgments

This work is an integral part of the PhD thesis of K.S. registered at the School of Informatics, Digital University Kerala, Trivandrum. We thank the Vice Chancellor of Digital University Kerala for institutional support. K.S. acknowledges funding from the ARTS-IRD grant, and both K.S. and M.L. acknowledge support from the South Pacific Community. Part of this work was funded by the Pacific-European Union Marine Partnership (PEUMP) Programme. Additional support was provided by the BRIDGES-AVATAR project, funded under the France 2030 programme (Grant Number ANR-22-EXBR-0004). I.S. acknowledges funding from CSIR, New Delhi, and the Deep Ocean Mission project GAP3631. We thank the World Climate Research Programme's Working Group on Coupled Modelling (WGCM), which is responsible for CMIP, and the climate modeling groups (listed in table S1) for producing and making their model outputs available. We are grateful for insightful discussions with Olivier Aumont and Thomas Gorgues. This is NIO contribution 7556.

Conflict of interest

The authors declare no conflicts of interest.

Data availability statement

The data that support the findings of this study are openly available at the following URL/DOI: https://zenodo.org/records/15804213.

Ethics statement

Not applicable.

Author contributions

Matthieu Lengaigne 0000-0002-0044-036X
Conceptualization (equal), Data curation (supporting), Funding acquisition (equal), Methodology (equal), Resources (equal), Supervision (equal), Writing – review & editing (equal)

Iyyappan Suresh 0000-0001-9049-5091
Funding acquisition (equal), Resources (equal), Software (equal), Supervision (equal), Writing – review & editing (equal)

Cyril Dutheil 0000-0001-6891-2389
Writing – review & editing (equal)

Jérôme Vialard 0000-0001-6876-3766
Conceptualization (equal), Supervision (equal), Writing – original draft (equal), Writing – review & editing (equal)

References

Anugerahanti P, Roy S and Haines K 2018 A perturbed biogeochemistry model ensemble evaluated against *in situ* and satellite observations *Biogeosciences* **15** 6685–711
Behrenfeld M J, O'Malley R T, Siegel D A, McClain C R, Sarmiento J L, Feldman G C, Milligan A J, Falkowski P G, Letelier R M and Boss E S 2006 Climate-driven trends in contemporary ocean productivity *Nature* **444** 752–5
Bopp L *et al* 2013 Multiple stressors of ocean ecosystems in the 21st century: projections with CMIP5 models *Biogeosciences* **10** 6225–45
Bopp L, Aumont O, Kwiatkowski L, Clerc C, Dupont L, Ethé C, Gorgues T, Séférian R and Tagliabue A 2022 Diazotrophy as a key driver of the response of marine net primary productivity to climate change *Biogeosciences* **19** 4267–85
Dong L, Zhou T and Wu B 2013 Indian Ocean warming during 1958–2004 simulated by a climate system model and its mechanism *Clim. Dyn.* **42** 203–17
Dunstan P K, Foster S D, King E, Risbey J, O'Kane T J, Monselesan D, Hobday A J, Hartog J R and Thompson P A 2018 Global patterns of change and variation in Sea surface temperature and chlorophyll a *Sci. Rep.* **8** 1–9
Eyring V, Bony S, Meehl G A, Senior C A, Stevens B, Stouffer R J and Taylor K E 2016 Overview of the coupled model intercomparison project phase 6 (CMIP6) experimental design and organization *Geosci. Model Dev.* **9** 1937–58 Dataset
Feng J, Lian T and Chen D 2023 Tropical Indian ocean mixed layer bias in CMIP6 CGCMs primarily attributed to the AGCM surface wind bias *J. Clim.* **36** 4169–88
Friedland K D, Stock C, Drinkwater K F, Link J S, Leaf R T, Shank B V, Rose J M, Pilskaln C H and Fogarty M J 2012 Pathways between primary production and fisheries yields of large marine ecosystems *PLoS One* **7** e28945
Gregg W W and Rousseaux C S 2014 Decadal trends in global pelagic ocean chlorophyll: a new assessment integrating multiple satellites, *in situ* data, and models *Journal of Geophysical Research: Oceans* **119** 5921–33
Gregg W W and Rousseaux C S 2019 Global ocean primary production trends in the modern ocean color satellite record (1998–2015) *Environ. Res. Lett.* **14** 124011
Gopika S, Sadhvi K, Vialard J, Danielli V, Neetu S and Lengaigne M 2025 Drivers of future Indian ocean warming and its spatial pattern in CMIP models *Earth's Future* **13** 1–22
Hammond M L, Beaulieu C, Henson S A and Sahu S K 2020 Regional surface chlorophyll trends and uncertainties in the global ocean *Sci. Rep.* **10** 15273
Held I M and Soden B J 2006 Robust responses of the hydrological cycle to global warming *J. Clim.* **19** 5686–99
Henson S A, Beaulieu C and Lampitt R 2016 Observing climate change trends in ocean biogeochemistry: when and where *Global Change Biol.* **22** 1561–71
Hood R R, Ummenhofer C C, Phillips H E and Sprintall J 2024 Introduction to the Indian ocean *The Indian Ocean and its Role in the Global Climate System* (Elsevier) pp 1–31
Kwiatkowski L *et al* 2020 Twenty-first century ocean warming, acidification, deoxygenation, and upper-ocean nutrient and primary production decline from CMIP6 model projections *Biogeosciences* **17** 3439–70
Lachkar Z, Lévy M and Smith S 2018 Intensification and deepening of the Arabian Sea oxygen minimum zone in response to increase in Indian monsoon wind intensity *Biogeosciences* **15** 159–86
Laufkötter C *et al* 2015 Drivers and uncertainties of future global marine primary production in marine ecosystem models *Biogeosciences* **12** 6955–84
Lecomte M, Rochette J, Laurans Y and Lapeyre R 2017 *Indian Ocean Tuna Fisheries:Between Development Opportunities and Sustainabilityissues* IDDRI
Lengaigne M *et al* 2024 An ocean-only framework for correcting future CMIP oceanic projections from their present-day biases *ESS Open Archive* 101023
Lévy M, Shankar D, André J M, Shenoi S S C, Durand F and de Boyer Montégut C 2007 Basin-wide seasonal evolution of the Indian Ocean's phytoplankton blooms *Journal of Geophysical Research: Oceans* **112**
Li G, Xie S P and Du Y 2015 Monsoon-induced biases of climate models over the tropical Indian Ocean *J. Clim.* **28** 3058–72

Li G, Xie S P, Du Y and Luo Y 2016 Effects of excessive equatorial cold tongue bias on the projections of tropical Pacific climate change. Part I: the warming pattern in CMIP5 multi-model ensemble *Clim. Dyn.* **47** 3817–31
Long S M, Li G, Hu K and Ying J 2020 Origins of the IOD-like biases in CMIP multimodel ensembles: the atmospheric component and ocean–atmosphere coupling *J. Clim.* **33** 10437–53
Modi A and Roxy M K 2023 Past trends and future projections of marine primary productivity in the tropical Indian ocean *Dynamics of Planktonic Primary Productivity in the Indian Ocean* (Springer International Publishing) pp 191–206
Moffett J W and Landry M R 2020 Grazing control and iron limitation of primary production in the Arabian Sea: implications for anticipated shifts in Southwest monsoon intensity *Deep Sea Res. Part II* **179** 104687
Mohanty S, Bhattacharya B and Singh C 2024 Spatio-temporal variability of surface chlorophyll and pCO2 over the tropical Indian Ocean and its long-term trend using CMIP6 models *Sci. Total Environ.* **908** 168285
Parvathi V, Suresh I, Lengaigne M, Izumo T and Vialard J 2017 Robust projected weakening of winter monsoon winds over the Arabian Sea under climate change *Geophys. Res. Lett.* **44** 9833–43
Pathirana G, Noh K M, Lee D G, Park H J, Wang D and Kug J S 2024 Intensified surface chlorophyll responses to the Indian ocean dipole under greenhouse warming *Environ. Res. Lett.* **19** 064072
Praveen V, Ajayamohan R S, Valsala V and Sandeep S 2016 Intensification of upwelling along Oman coast in a warming scenario *Geophys. Res. Lett.* **43** 7581–9
Praveen V, Valsala V, Ajayamohan R S and Balasubramanian S 2020 Oceanic mixing over the northern Arabian sea in a warming scenario: tug of war between wind and buoyancy forces *J. Phys. Oceanogr.* **50** 945–64
Resplandy L, Lévy M, Madec G, Pous S, Aumont O and Kumar D 2011 Contribution of mesoscale processes to nutrient budgets in the arabian sea *Journal of Geophysical Research: Oceans* **116**
Roxy M K, Modi A, Murtugudde R, Valsala V, Panickal S, Prasanna Kumar S, Ravichandran M, Vichi M and Lévy M 2016 A reduction in marine primary productivity driven by rapid warming over the tropical Indian Ocean *Geophys. Res. Lett.* **43** 826–33
Sathyendranath S *et al* 2018 ESA ocean colour climate change initiative (Ocean_Colour_cci): Version 3.1 data *Centre for Environmental Data Analysis* [Dataset] (https://doi.org/10.5285/9c334fbe6d424a708cf3c4cf0c6a53f5)
Seelanki V and Pant V 2021 Diversity in the simulation of chlorophyll concentration by CMIP5 earth system models over the Indian ocean *Mar. Geod.* **44** 505–30
Sharma S, Ha K J, Cai W, Chung E S and Bódai T 2022 Local meridional circulation changes contribute to a projected slowdown of the Indian Ocean Walker circulation *npj Climate and Atmospheric Science* **5** 15
Siegel D A *et al* 2013 Regional to global assessments of phytoplankton dynamics from the Seawifs mission *Remote Sens. Environ.* **135** 77–91
Sooraj K P, Terray P and Mujumdar M 2014 Global warming and the weakening of the Asian summer monsoon circulation: assessments from the CMIP5 models *Clim. Dyn.* **45** 233–52
Suresh I, Vialard J, Lengaigne M, Izumo T, Parvathi V and Muraleedharan P M 2018 Sea level interannual variability along the west coast of India *Geophys. Res. Lett.* **45** 12–440
Tagliabue A, Barrier N, Du Pontavice H, Kwiatkowski L, Aumont O, Bopp L, Cheung W W, Gascuel D and Maury O 2020 An iron cycle cascade governs the response of equatorial Pacific ecosystems to climate change *Global Change Biol.* **26** 6168–79
Tagliabue A, Kwiatkowski L, Bopp L, Butenschön M, Cheung W, Lengaigne M and Vialard J 2021 Persistent uncertainties in ocean net primary production climate change projections at regional scales raise challenges for assessing impacts on ecosystem services *Frontiers in Climate* **3** 738224
Tian F and Zhang R H 2023 Decreasing surface chlorophyll in the tropical ocean as an indicator of anthropogenic greenhouse effect during 1998–2020 *Environ. Res. Lett.* **18** 084019
Tian F and Zhang R H 2024 Emerging hotspots of surface chlorophyll trend in the tropical oceans *Journal of Geophysical Research: Oceans* **129** e2023JC020681
Vecchi G A, Soden B J, Wittenberg A T, Held I M, Leetmaa A and Harrison M J 2006 Weakening of tropical Pacific atmospheric circulation due to anthropogenic forcing *Nature* **441** 73–6
Wiggert J D, Hood R R, Banse K and Kindle J C 2005 Monsoon-driven biogeochemical processes in the Arabian Sea *Prog. Oceanogr.* **65** 176–213
Yu S, Bai Y, He X, Gong F and Li T 2023 A new merged dataset of global ocean chlorophyll-a concentration for better trend detection *Frontiers in Marine Science* **10** 1051619
Zhuo J Y, Lee C Y, Sobel A, Seager R, Camargo S J, Lin Y H and Reed K A 2025 A more la Niña–like response to radiative forcing after flux adjustment in CESM2 *J. Clim.* **38** 1037–50